Ravi Kumar, R. Mager, F. Phillipp, A. Zimmermann[a], G. Rixecker[a]

Max-Planck-Institut für Metallforschung and Institut für Nichtmetallische Anorganische Materialien, Universität Stuttgart, Pulvermetallurgisches Laboratorium, Stuttgart, Germany

[a] Robert Bosch GmbH, Corporate Research and Advance Engineering, Stuttgart, Germany

High-temperature deformation behavior of nanocrystalline precursor-derived Si–B–C–N ceramics in controlled atmosphere

Dedicated to Professor Dr. Fritz Aldinger on the occasion of his 65th birthday

In precursor-derived nanocrystalline Si–B–C–N materials, grain or interphase boundaries constitute a major part of the material. They control various properties of nanostructured solids, e. g., by forming fast diffusion pathways. In such highly covalent materials, where the interfaces between the individual crystallites or domains tend to be broadened and structurally disordered, high-temperature plastic deformation (i. e., the creep behavior) can be used as a probe which is particularly sensitive to processes involving internal interfaces and glass-like features of the microstructure. The focus of the present study is an investigation of the deformation behavior of precursor-derived nanocrystalline Si–B–C–N ceramics in the phase-separated amorphous and nanocrystalline states under inert atmospheres. A concise analysis of creep mechanisms free of any oxidation effects was carried out. Isothermal compression creep experiments at 1400 °C and at various loads (50 MPa–150 MPa) have indicated a stress exponent near to unity hinting diffusion creep, and an activation energy of 0.16 ± 0.03 MJ/mol was derived from temperature change experiments under an iso-stress condition. The mechanisms of deformation are elucidated using a free volume model.

Keywords: Si–B–C–N ceramics; Free volume; TEM; Compression creep

1. Introduction

Precursor-derived Si–B–C–N ceramics are a new class of high-temperature structural ceramics produced from solid-state thermolysis of polymers. They are of interest, since the properties of the material can be tailored at the atomic/molecular level [1]. High-temperature stability up to 2000 °C [1–5], chemical and mechanical stability at elevated temperatures concurrent with high creep resistance [6–12] induce continued scientific interest in this class of materials. Si–B–C–N ceramics obtained from boron modified poly(vinyl)silazanes with chemical compositions of $(B[C_2H_4–Si(CH_3)NH]_3)_n$ (denoted T2-1) and $(B[C_2H_4–Si(H)NH]_3)_n$ (denoted MW-33) were investigated extensively for their high-temperature mechanical properties in atmospheric conditions.

Polymer-derived Si–B–C–N ceramics in the amorphous state as well as in the crystalline state exhibit extraordinary creep resistance. Si–B–C–N ceramics in the amorphous state (MW-33 and T2-1) exhibited low strain rates in the order of 10^{-8} s^{-1} with no sign of steady state even after 300 h of testing [8]. In the crystalline state, annealed MW-33-derived ceramics heat-treated at 1800 °C for 3 h in 1 MPa N_2 atmosphere exhibited an order of magnitude increase in creep resistance for the same combination of load and temperature (1400 °C, 100 MPa). The strain rates of such annealed Si–B–C–N ceramics continued to decrease and exhibited values in the range of 10^{-9} s^{-1} at the end of 300 h of creep [11, 12].

T2-1-derived ceramics annealed under identical conditions, but synthesized using larger polymer particle size fractions, showed a relatively lower creep resistance in contrast to their crystalline MW-33 counterparts as a result of extensive internal oxidation of the material [13]. Extensive internal oxidation due to relatively wide-spaced pore channels converted the highly covalent, creep-resistant non-oxidic microstructure to one containing a substantial amount of oxidic phase, albeit low strain rates in the order of 10^{-8} s^{-1} were observed for the most critical conditions of creep [13].

In the present investigation, we have chosen T2-1-derived materials with identical composition, and annealing conditions similar to those investigated in air which were subjected to severe oxidation. The focus of the present study is to understand the material behavior at elevated temperatures under argon atmosphere so that a concise analysis of the deformation mechanisms of these materials can be made without any oxidation- induced effects on the creep behavior.

2. Experimental

The synthesis of the polymer precursor with the chemical composition $(B[C_2H_4–Si(CH_3)NH]_3)_n$ and details of the ceramization processes can be found elsewhere [2, 14]. Nano-crystalline Si–B–C–N ceramics were prepared by annealing the polymer-derived amorphous Si–B–C–N ceramics in nitrogen atmosphere of 1 MPa at a temperature of 1800 °C for a duration of 3 h in a high-temperature fur-

Table 1. Chemical analysis of the crystalline T2-1 derived Si–B–C–N ceramic prior to creep investigations. (XRF = X-ray fluorescence, ICP-OES = Inductively coupled plasma-optical emission spectroscopy, Vario and TC-436 are combustion techniques).

Element	% Mass	Process
Si	45.1	XRF
B	6.0	ICP-OES
C	30.5	Vario
N	17.5	Vario
O	1.1	TC-436

nace (FCT, Germany). Transformation of the Si–B–C–N ceramics from the amorphous to the crystalline state was accompanied by a weight loss of 3.0 % and an increase in bulk density of 8.8 %. The bulk density of the crystalline Si–B–C–N ceramic measured by displacement measurements in mercury is 1.93 g/cm^3.

Chemical analysis of the sample was carried out by spectroscopic methods and the elemental composition is listed in Table 1. The elements carbon, nitrogen, and oxygen were determined by combustion techniques using Elementar Vario EL and LECO TC-436. Boron was quantified by inductively coupled plasma-atomic emission spectroscopy (ICP-AES) using an ISA JOBIN YVON JY70 plus instrument. X-ray fluorescence was used to quantify silicon in these ceramic materials. The empirical chemical formula of the ceramic is found to be $Si_{2.9}\ B_{1.0}\ C_{4.6}\ N_{2.3}$, which is deduced from the elemental composition.

The X-ray diffraction measurements were carried out at room temperature on a Siemens D5000 X-ray diffractometer with a position-sensitive detector. The voltage and current used for the measurements were 40 kV and 30 mA, respectively. The samples used for the TEM experiments were prepared following standard techniques, which involve diamond cutting, ultrasonic drilling, mechanical grinding, dimpling, polishing, and argon-ion thinning to perforation. TEM measurements at room temperature were made using a Zeiss EM 912 microscope at an operating voltage of 120 kV.

Compression-creep specimens were prepared by cutting and grinding the annealed samples. For carrying out compression-creep experiments in a controlled atmosphere, a test frame 'Zwick' with a furnace from the company 'Maytec' was used as shown in Fig. 1. Two thermocouples (Pt/Pt 10 % Rh) are installed inside the furnace, one for measuring the temperature of the sample and connected to the controller to maintain the creep test temperature, and the other for limiting the temperature to 1530 °C. The heating elements and the radiation shields are made of molybdenum (Fig. 1). A rotary-vane vacuum pump in series with a turbomolecular pump which can generate vacuum of the order of 9×10^{-6} mbar is used for the evacuation of the chamber. The vacuum generated in the chamber is constantly monitored using a Penning gauge. A 10 kN load cell is installed in the machine, although the frame itself is designed for 100 kN. The load measurement accuracy is of the order of ± 0.2 N. During all the creep tests, a continuous flow of argon gas with a flow rate of 1 litre/min is maintained.

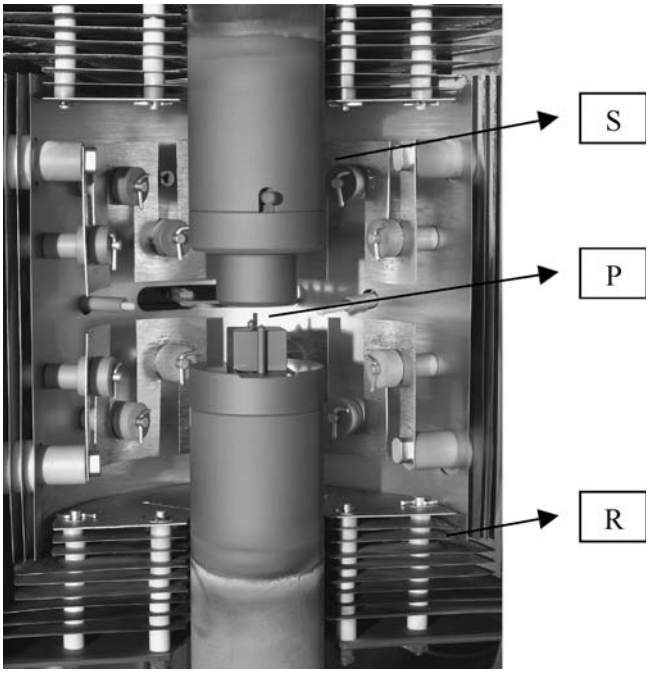

Fig. 1. Experimental set-up for compression creep showing the sample (**P**) placed between two SiC pads (**S**). Heating and radiation shields are made of molybdenum (**R**).

3. Results

Earlier studies on structural characterization of crystallized Si–B–C–N ceramic samples of MW-33 and T2-1-derived materials indicated that the resulting nanostructure is dependent on the actual annealing conditions [12, 14]. The annealing temperature, holding time, and nitrogen pressure control the size, distribution, and morphology of the crystallites formed in situ in the matrix. A pronounced influence of the size of the polymer particles used for processing on the crystallization behavior is also observed [14]. However, for the present investigation only a brief note on the structural features of the material under investigation is given via results obtained from X-ray diffraction (XRD) and transmission electron microscopy (TEM).

X-ray diffraction patterns were recorded as shown in Fig. 2. The concomitant bright-field TEM image shows the

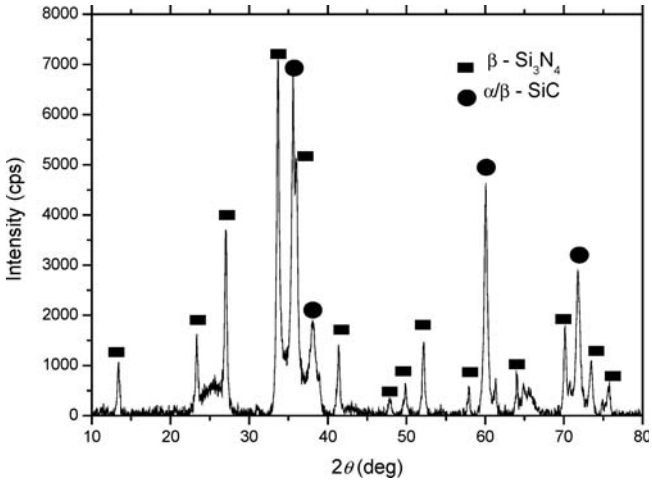

Fig. 2. X-ray diffraction diagram of the T2-1-derived crystalline Si–B–C–N ceramic annealed at 1800 °C (3 h, 1 MPa N_2 atmosphere) showing peaks corresponding to SiC and Si_3N_4 crystallites.

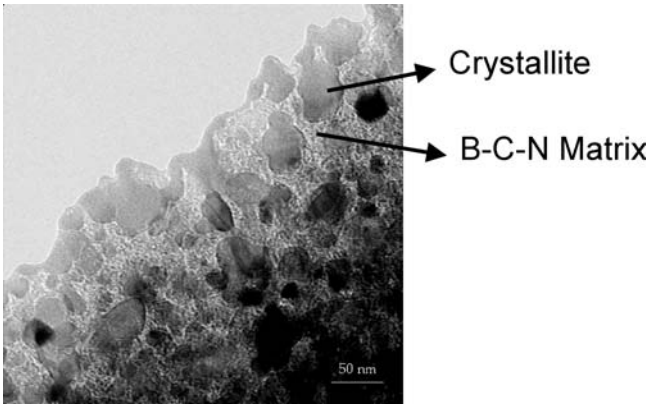

Fig. 3. Bright-field image of the T2-1-derived crystalline Si–B–C–N ceramic showing nanocrystallites dispersed in a matrix of B–C–N.

structural features of the crystallized samples (Fig. 3). The Bragg reflections correspond to SiC and β-Si_3N_4. A broad peak corresponding to $2\theta = 25°–26°$ indicates the presence of turbostratic BN and C. An analogous observation is made by TEM, where the bright-field image (Fig. 3) distinctly shows the formation of crystallites of SiC and Si_3N_4. The average size of the crystallites was found to be around 30–50 nm. They were dispersed in a matrix of boron, nitrogen, and carbon (B–C–N matrix) which is amorphous. However, the amorphous nature of the matrix is still not very clear.

3.1. Time dependence of deformation

The time dependence of deformation of T2-1-derived crystalline Si–B–C–N ceramics investigated in compression creep under isothermal tests at a temperature of 1400 °C and compressive stresses 50, 100, and 150 MPa is depicted in Fig. 4. The strain rates decrease with time at all loads during the entire duration of the creep test with no asymptotic approach to steady state. This behavior indicates a continuous increase in creep resistance with time. Since no drastic change in the microstructures of the specimens investigated is expected as a result of an inert atmosphere, valid creep parameters can be evaluated using the well known Norton equation for compression creep which is given in Eq. 1 [8]:

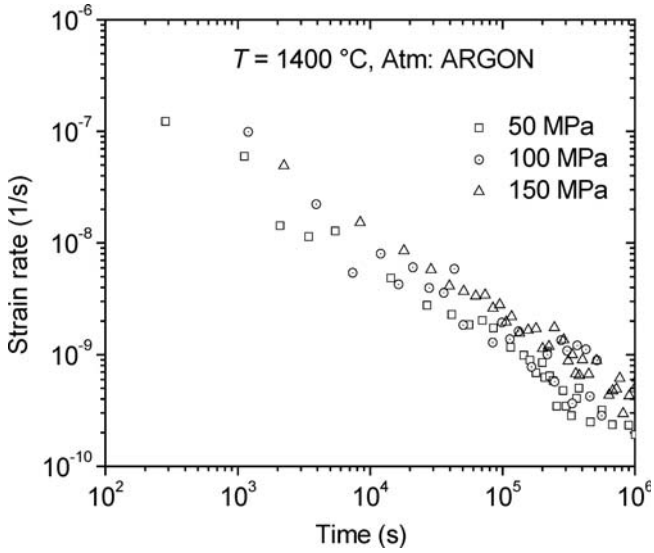

Fig. 4. Variation of strain rates with time and applied compressive stresses during isothermal creep experiments with T2-1-derived crystalline Si–B–C–N ceramics at 1400 °C.

$$\dot{\varepsilon} = A \cdot \sigma^n \cdot \exp\left(\frac{-Q}{R \cdot T}\right) \cdot t^{-c} \quad (1)$$

where A is a constant which is representative of the microstructural state of the material, σ is the compressive stress, Q is the activation energy for creep, R is the gas constant, T is the absolute temperature, t is the creep time, c is the time exponent, and n is the stress exponent. It is obvious that the minimum strain rates are obtained at the end of the creep tests, and hence the creep parameters (n and Q) are determined using strain rate values at time, $t = 300$ h ($\approx 10^6$ s). No noticeable change in the slope of the curves could be identified, and a time exponent of $c \approx 0.73$ was determined which did not change significantly during the entire creep test.

3.2. Stress dependence of deformation

The compression-creep experiments carried out at a constant temperature of 1400 °C for various loads from 5–100 MPa showed a maximum deformation of around 1.6 %–1.7 % after 300 h for T2-1-derived crystalline materials annealed at 1900 °C, tested in air [11]. The strain rates achieved at the end of the creep tests were of the order of $4 \times 10^{-9}\ s^{-1}$ to $5 \times 10^{-9}\ s^{-1}$. Contrarily, in argon atmosphere, crystalline T2-1-derived material exhibited far less accumulated viscous deformation at the end of the creep tests and low deformation rates. The total viscous deformation exhibited in the load regime (50–150 MPa), varied between about 0.32 % and 0.54 %, which was in fact dependent on the applied compressive stress during the isothermal test (T = 1400 °C). The strain rates at the lowest and highest loads investigated during the isothermal tests reached values in the order of $2 \times 10^{-10}\ s^{-1}$ to $4 \times 10^{-10}\ s^{-1}$ after 300 h of creep time as shown in Fig. 4. For all the three loads only an extended primary creep stage over the entire test duration was observed (Fig. 4).

3.3. Temperature dependence of deformation

The deformation behavior of T2-1-derived crystalline Si–B–C–N ceramics as a function of temperature was studied by performing a temperature change experiment during an iso-stress condition at 100 MPa (Fig. 5). The specimen was initially subjected to a temperature of 1300 °C for a period of 100 h. Subsequently the temperature was raised to 1400 °C and 1500 °C, keeping the compressive stress constant through out the experiment and allowing the material to creep at all the three temperatures. Another sample from the same material was simultaneously tested in air at 1500 °C coupled with a compressive load of 100 MPa in another creep machine and the strain values are plotted for comparison in Fig. 5. The deformation recorded after 250 h was around 0.5 % and around 2.3 % for tests carried out in argon and in air respectively. The material tested in air, however, failed at the end of around 260 h with a strain to failure of 2.45 %.

The deformation rates corresponding to different temperatures are plotted as a continuous function of time in

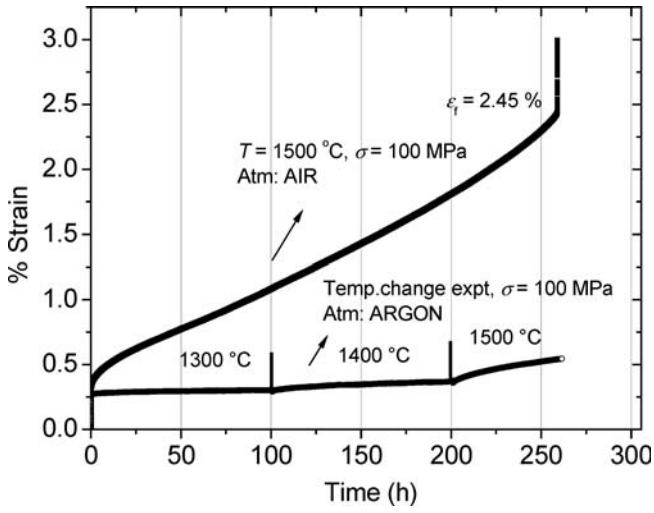

Fig. 5. Deformation of the crystalline T2-1-derived Si–B–C–N ceramic during a temperature change experiment at a constant compressive stress of 100 MPa. Deformation behavior of the same material at a temperature of 1500 °C and a compressive stress of 100 MPa in atmospheric ambience is given for comparison.

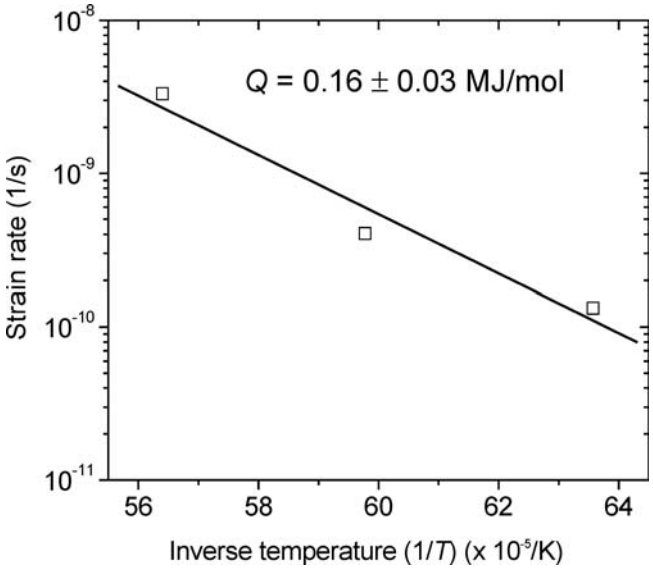

Fig. 7. Arrhenius plot for the calculation of the activation energy of the deformation rate of crystalline T2-1 derived Si–B–C–N ceramic after 10^6 s. All tests were performed at a stress of 100 MPa.

Fig. 6. A strong temperature dependence of strain rates at all times was observed and it can be seen that the dependence was the same at all times. An affine inverse linear function which is deduced from free-volume theory was fitted to the experimental data. The extrapolated strain rate values at $t = 10^6$ s for all the three different temperatures investigated are plotted against reciprocal temperature (Fig. 7) and the activation energy in the temperature regime of 1300 °C to 1500 °C is determined to be $Q = 0.16 \pm 0.03$ MJ/mol.

4. Discussion

4.1. Time and stress dependence of the deformation rate

High-temperature deformation studies by compression creep in atmospheric ambience for amorphous and crystalline Si–B–C–N ceramics exhibited a similar time dependence of strain rates [8, 11, 12]. A continuous decrease in strain rates with time was observed, indicating only the primary stage of creep for the entire creep tests for all loads in the temperature regime investigated [8, 11, 12]. However, crystalline T2-1-derived Si–B–C–N ceramics produced by heat treatment at 1800 °C (3 h, 1 MPa N_2 pressure), investigated in air at compressive stresses from 25 to 150 MPa, and at temperatures from 1350 °C to 1500 °C, exhibited increasing strain rates beyond 2×10^5 s [13]. The creep behavior was extensively influenced by oxidation and the non-oxide covalent microstructure was converted to that of an oxidic one, resulting in decreasing creep resistance with time and temperature. Microstructural investigations elucidating this behavior and the role of oxidation on the high-temperature deformation behavior are explained in detail elsewhere [13]. However, the crystalline T2-1-derived material synthesized under identical conditions, i. e., heat treated at 1800 °C (3 h, 1 MPa N_2 pressure), when investigated in argon atmosphere showed only primary creep for the entire duration of the creep test, as shown in Fig. 4. This indicates an entirely different behavior in an oxygen-free environment. As a result of an inert atmosphere during the creep tests, the mechanisms of deformation of these materials were determined unambiguously.

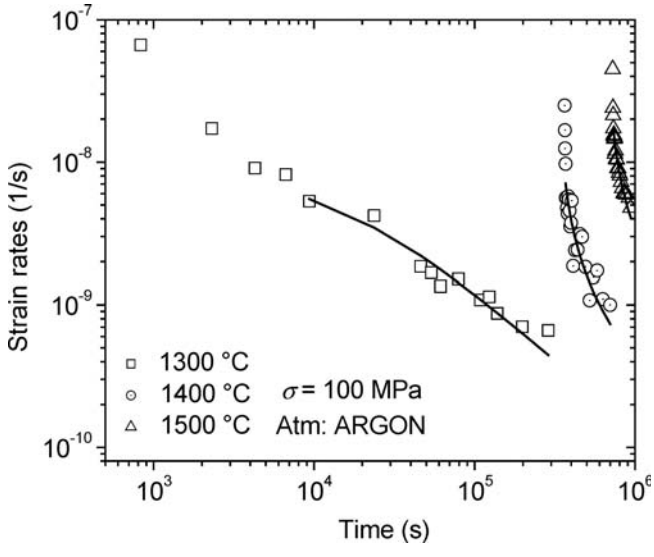

Fig. 6. Variation of strain rates relative to time at 100 MPa and different temperatures during iso-stress creep experiments with T2-1 derived crystalline Si–B–C–N ceramics.

The time dependence of the deformation rate for the T2-1-derived nanocrystalline Si–B–C–N ceramics can be understood on the basis of a continuous structural evolution of the matrix phase during deformation. Since the time dependence is similar to that of its amorphous counterpart [8], it is reasonable to assume that the matrix – consisting of well-defined but only partially crystalline SiC, Si_3N_4, BN domains and amorphous, graphite-like regions – plays the dominant role for the deformation behavior even of the crystalline Si–B–C–N ceramic rather than the dispersed nanocrystallites. In close analogy to the amorphous sample [8], it is the ongoing structural alteration in the amorphous matrix with testing time which is responsible for the continuous reduction of the deformation rate of the partially crystalline ceramics.

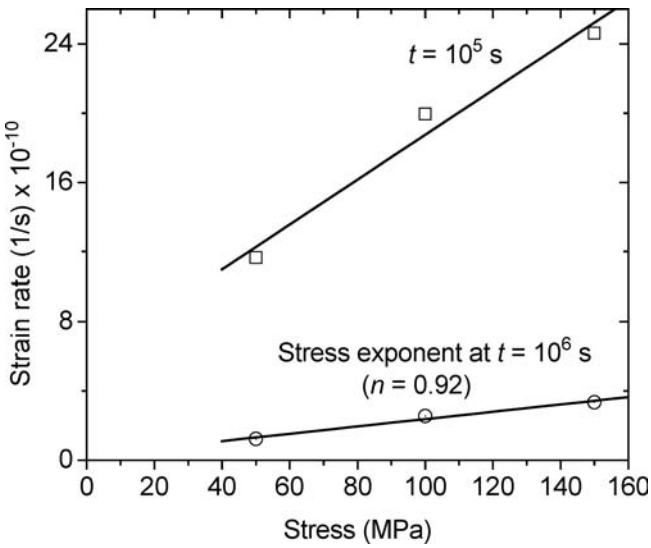

Fig. 8. Strain rate as a function of stress at 1400 °C for T2-1-derived crystalline Si–B–C–N ceramic after 10^5 s and 10^6 s and calculation of stress exponent.

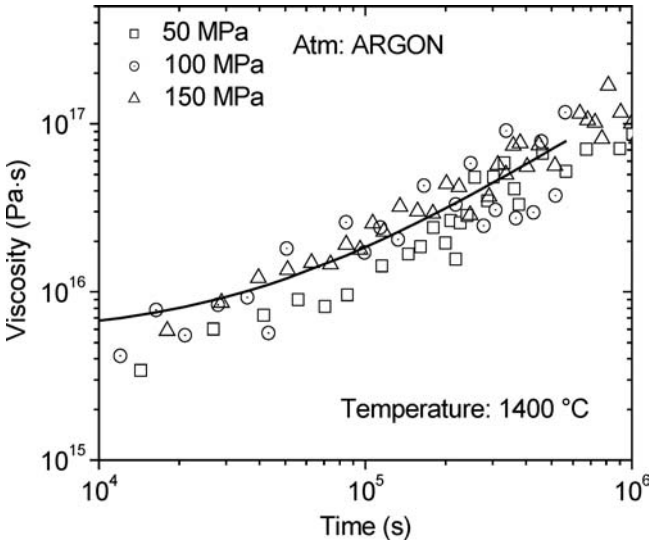

Fig. 9. Measured data and fitted curve of the time dependent viscosity of the T2-1- derived crystalline Si–B–C–N ceramic.

The stress dependence of the deformation rate is shown in Fig. 8a for two different testing times, that is, after 10^5 s and 10^6 s. A linear fit to the experimental data describes the stress dependence of deformation rate very well. The stress exponent was calculated by plotting the minimum strain rates obtained during the creep tests (i.e after 10^6 s) against stress as shown in Fig. 8b. The slope of the linear fit to the experimental data gives a value near to unity indicating a diffusion-based mechanism of creep. The atomistic mechanisms of viscous flow even of the crystalline materials can be explained using the free volume theory, which was applied to understand the deformation mechanisms in metallic glasses [15–17] and recently in amorphous Si–B–C–N ceramics [8]. In the following two sections, the time and temperature dependence of viscosity is analyzed using the aforementioned theory.

4.2. Time dependence of viscosity

Figure 9 shows the time-dependent increase in viscosity that was calculated using Eq. 2 for the T2-1-derived crystalline ceramic at a temperature of 1400 °C and various applied stresses. The strain rates for the calculation of the viscosity are obtained from Fig. 4.

$$\eta = \frac{\sigma}{3 \cdot \dot{\varepsilon}} \tag{2}$$

A linear expression as given in Eq. 3 was used to fit the experimental data in Fig. 9.

$$\eta(t) = a + b \cdot t \tag{3}$$

where a and b are constants, and t is the creep time.

The fitted data and experimental data are in good accordance with each other, however, at shorter times ($< 2 \times 10^4$ s) a deviation is observed which is attributed to anelastic deformation. Independent of the applied stress (σ), the values of viscosity increase linearly and reach the order of 10^{17} Pa · s at the end of creep time, $t = 10^6$ s. Within the time frame of creep testing, more than 2 orders of magnitude increase in viscosity is observed. Qualitatively, the behavior is similar to their amorphous and MW-33-derived crystalline counterparts investigated in air, where a similar linear time dependence has been observed [8, 11, 18]. However, T2-1-derived materials which were extensively influenced by oxidation did not show such linear time dependence for long durations [13]. In an oxidation-free environment, T2-1-derived crystalline materials not only showed a continuous increase of viscosity during 300 h of testing time, but also an order of magnitude increase in the values at any instant of time in comparison with materials investigated in air. The similar time-dependent increase both in the case of amorphous materials and in crystalline materials is indicative of the fact that the role of crystallites in the crystalline state of such materials is of minor importance. However, the increase in viscosity of the surrounding matrix in crystalline materials should be the reason for the higher values reported here. The disordered turbostratic matrix that surrounds the crystallites (as observed in Fig. 3) is still amorphous, and continuous annihilation of defects in the residual amorphous phase causes such increasing viscosity values.

The annihilation of defects during structural relaxation takes place by a bimolecular process, which means that the annihilation of free volume takes place by the collapse of two adjacent free volume fluctuations [17, 19, 20]. Hence the annihilation rate can be written as

$$\frac{\mathrm{d}c_\mathrm{f}}{\mathrm{d}t} = -k_\mathrm{r} c_\mathrm{f}^2 \tag{4}$$

where c_f is the concentration of flow defects, and k_r is a rate constant. The annihilation kinetics follows from the observed linear increase of viscosity with time as seen in Fig. 9. Also, from the free-volume theory, in the low-stress regime, the viscosity is given by

$$\eta = \frac{kT\Omega}{c_\mathrm{f} k_\mathrm{r} (\varepsilon_0 v_0)^2} \tag{5}$$

where k is the Boltzmann constant, T is the creep test temperature, Ω is the atomic volume, and v_0 is the volume which undergoes a strain ε_0 under the application of an external stress σ.

The solution of the differential equation (Eq. 4) gives the value of the concentration of flow defects c_f. Incorporation of this value into Eq. 5 leads to an affine linear relation of viscosity with time which takes the form of Eq. 3. Hence, the time dependence of viscosity can be very well described by the free-volume model.

4.3. Temperature dependence of viscosity

Viscosities calculated from strain rates (see Fig. 6 for the strain rate values) corresponding to three different test temperatures in a temperature change experiment at a constant applied stress of 100 MPa using Eq. 2 are plotted in Fig. 10 as a function of time. A linear and distinct dependence of viscosity during the entire test time for all temperatures was observed. An order of magnitude decrease in the viscosity values from 10^{17} Pa · s to 10^{16} Pa · s was observed with increase in test temperature to 1500 °C at the end of the creep test. The dotted line in Fig. 10 represents the expected slope according to Eq. 3, and is valid for all the three test temperatures investigated. However, even at the severe combination of load and temperature, the viscosity values were increasing at the end of the creep test. This supports the fact that even under these extreme creep conditions, the highly covalent, load-carrying bridges of the material are not softened, indicating very high creep resistance.

5. Conclusions

Annealed nanocrystalline T2-1-derived Si–B–C–N ceramics were investigated for their high-temperature mechanical properties in argon atmosphere. In this work, the influence of the interfaces in these nano-structured materials was studied using creep measurements as a probe. The investigation in controlled atmosphere showed a dramatic increase in creep resistance (strain rates $\sim 10^{-10}$ s^{-1}) in contrast to the results obtained in atmospheric conditions. The existence of only an extended primary regime of creep with no asymptotic approach to steady state for the entire creep tests indicates the role of the matrix phase only (lack of long-range order, annihilation of defects) on the high-temperature deformation. A free-volume model was successfully used to analyze the deformation behavior of the crystalline state. A stress exponent near unity indicates a diffusion creep mechanism.

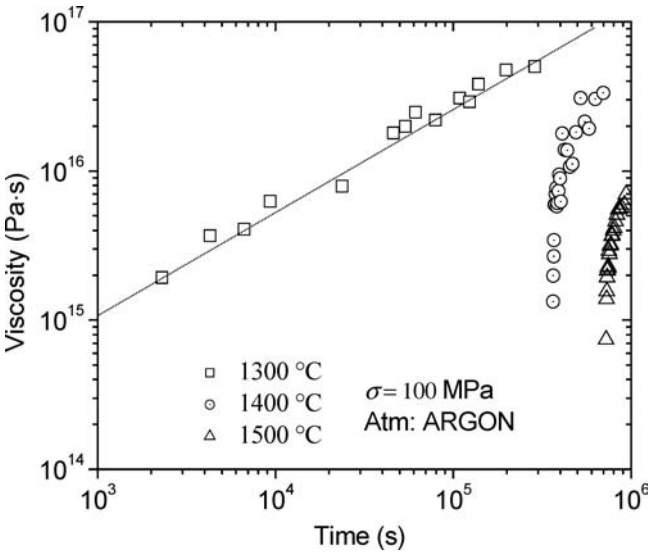

Fig. 10. Variation of viscosity of the T2-1 derived crystalline Si–B–C–N ceramic with time and temperature. All tests performed at a constant compressive stress of 100 MPa.

The Graduiertenkolleg Innere Grenzflächen (GKIG) under the Deutsche Forschungsgemeinschaft (DFG) and its chairman Prof. Rühle are gratefully acknowledged for the financial support. Prof. Aldinger is thanked for his constant encouragement and the fruitful discussions we had with him during the course of this work. Mr. Hahn, Mr. Kaiser, and Ms. Thomas are thanked for the technical support.

References

[1] J. Bill, F. Aldinger: Adv. Mater. 7 (1995) 775.
[2] R. Riedel, A. Kienzle, W. Dreßler, L.M. Ruswisch, J. Bill, F. Aldinger: Nature (London) 382 (1996) 796.
[3] A. Müller, P. Gerstel, M. Weinmann, J. Bill, F. Aldinger: J. Eur. Ceram. Soc. 20 (2000) 2655.
[4] A. Müller, P. Gerstel, M. Weinmann, J. Bill, F. Aldinger: J. Eur. Ceram. Soc. 21 (2001) 2171.
[5] Z.-C. Wang, F. Aldinger, R. Riedel: J. Am. Ceram. Soc. 84 (2001) 2179.
[6] L. An, R. Riedel, C. Konetschny, H.-J. Kleebe, R. Raj: J. Am. Ceram. Soc. 81 (1998) 1349.
[7] R. Riedel, L.M. Ruschwisch, L. An, R. Raj: J. Am. Ceram. Soc. 81 (1998) 3341.
[8] M. Christ, G. Thurn, M. Weinmann, J. Bill, F. Aldinger: J. Am. Ceram. Soc. 83 (2000) 3025.
[9] M. Christ, A. Zimmermann, A. Zern, M. Weinmann, F. Aldinger: J. Mater. Sci. 36 (2001) 5767.
[10] A. Bauer, M. Christ, Y. Cai, A. Zimmermann, F. Aldinger (accepted for publication in J. Am. Ceram. Soc).
[11] R. Kumar, R. Mager, Y. Cai, A. Zimmermann, F. Aldinger: Scripta Mater. 51 (2004) 65.
[12] R. Kumar, S. Prinz, Y. Cai, A. Zimmermann, F. Berger, K. Müller, F. Aldinger: Acta Mater. 53 (2005) 4567.
[13] R. Kumar: Dissertation, Universität Stuttgart (2005).
[14] R. Kumar, P. Gerstel, Y. Cai, G. Rixecker, F. Aldinger: (accepted for publication in J. Mater. Sci).
[15] F. Spaepen, in: R. Balian, M. Kléman, J.-P. Poirier (Eds.), Physics of Defects, North-Holland, Amsterdam (1981) 134.
[16] M.H. Cohen, D. Turnbull: J. Chem. Phys. 31 (1959) 1164.
[17] M. Heggen, F. Spaepen, M. Feuerbacher: Mater. Res. Soc. Symp. Proc. 806 (2004) MM7.2.1.
[18] A. Zimmermann, A. Bauer, M. Christ, Y. Cai, F. Aldinger: Acta Mater. 50 (2002) 1187.
[19] A.I. Taub, F. Spaepen: Acta Metall. 28 (1980) 1781.
[20] F. Spaepen: Mater. Sci. Eng. A179/180 (1994) 81.

(Received November 15, 2005; accepted February 10, 2006)

Correspondence address

Dr. rer. nat. Ravi Kumar
Max-Planck-Institut für Metallforschung and
Institut für Nichtmetallische Anorganische Materialien
Universität Stuttgart, Pulvermetallurgisches Laboratorium
Heisenbergstr. 5, D-70569 Stuttgart, Germany
Tel.: +49 711 689 3108
Fax: +49 711 689 3131
E-mail: kumar@mf.mpg.de